Zgórecka et al.
Medical Journal of Cell Biology 2022
DOI: 10.2478/acb-2022-0024
Received: 20.10.22
Accepted: 14.11.22

Human ovarian follicular granulosa cells isolated during ART procedure reflect substantial changes in activation of hormonal signaling pathways, during long-term in vitro conditions

Wiktoria Zgórecka[1], Małgorzata Blatkiewicz[2], Maurycy Jankowski[2,3], Wiesława Kranc[1], Artur Bryja[1], Maciej Brązert[4], Błażej Chermuła[4], Wojciech Pieńkowski[5], Leszek Pawelczyk[4], Paul Mozdziak[6,7]

Abstract

The ovary is commonly known as an endocrine gland responsible for sex steroid production. One of the outstanding cells in ovarian microenvironment - granulosa cells (GCs) are responsible for converting the androgens to estrogens during follicular growth and secreting progesterone after ovulation. These secretory processes within the ovary are directly involved in hormonal signaling pathways, and they depend on different stages of cholesterol and lipid biosynthesis during the ovarian cycle. The understating of the regulation and further investigation into the processes taking part in ovary will expose new clinical advantages in detection and treatment of female reproductive system diseases associated with sex hormone abnormalities. The expression of genes belonging to ontology groups associated with steroid biosynthesis and metabolism, such as "cholesterol biosynthetic process" (GO:0006695, "regulation of lipid biosynthetic process" (GO:0046890), "regulation of lipid metabolic process" (GO:0019216), "response to insulin" (GO:0032868) and "response to lipopolysaccharide" (GO:0032496) were analyzed by using the microarray approach. The patterns of gene expression in human GCs at days 1-day, 7-day, 15-day, and 30-day of primary in vitro culture have been analyzed. Based on the microarray results, a group of upregulated genes have been selected: CCL20, CXCL5, STAR, MSMO1, and AADAC. The genes STAT5B, OPA3, PPARG, PROX1, and SEC14L2 were decreased across all the experimental groups during the 30-day cell cultivation period. These results suggest that, the GCs in cell culture under in vitro express steroidogenic markers and it is important to understand associations with lipid and liposaccharide synthesis relative to reproductive medicine.

Running title: Granulose cells – ART procedure

Keywords: granulosa cells (GCs), hormone, molecular pathway, cholesterol, lipid, metabolism, steroidogenesis

[1]Department of Anatomy, Poznan University of Medical Sciences, Poznań, Poland
[2]Department of Histology and Embryology, Poznan University of Medical Sciences, Poznań, Poland
[3]Department of Computer Science and Statistics, Poznan University of Medical Sciences, Poznań, Poland
[4]Department of Diagnostic and Treatment of Infertility, Department of Gynecological Endocrinology and Infertility Treatment Karol Marcinkowski University, Poznan University of Medical Sciences, Poznań, Poland
[5]Division of Perinatology and Women's Diseases, Poznan University of Medical Sciences, Poznań, Poland
[6]Physiology Graduate Program, North Carolina State University, Raleigh, NC, USA
[7]Prestage Department of Poultry Sciences, North Carolina State University, Raleigh, NC, USA
***Correspondence:** wkranc@ump.edu.pl
Full list of author information is available at the end of article

sciendo

Introduction

The most important function of the ovary as an endocrine gland is the production of sex steroid hormones to trigger follicular development, and ovulation. The follicle microenvironment in ovary can be described as a complex biological bi-directional system including oocytes, theca cells, granulosa cells (GCs), cumulus cells, and immune cells [1,2]. The key role in follicular processes take part two primary specialized steroidogenic cells. Theca interna layer of ovarian follicle consists of theca cells responsible for androgen synthesis [3]. The GCs are responsible for converting the androgens to estrogens during follicular growth and secreting the progesterone after ovulation, through corpus luteum [4].

The crucial compartment of the cells, mitochondria are the central sites for steroid hormone biosynthesis. The steroid hormones are derived from cholesterol and can be limited and have an impact on hormonal signaling pathways [5,6]. Studies based on mammals provided knowledge that lipid metabolites are donors od sufficient energy for morphological development and cell signaling processes during folliculogenesis. The fluctuations between lipids exploitation and storage by cells might cause oxidative stress and they may have influence on maintaining of follicular microenvironment homeostasis [1,2,7].

The main aim of this study was to highlight the expression and correlations of genes involved in several gene ontologies "cholesterol biosynthetic process (GO:0006695)", "regulation of lipid biosynthetic process (GO:0046890)", "regulation of lipid metabolic process (GO:0019216)", "response to insulin (GO:0032868)" and response to lipopolysaccharide (GO:0032496)". The identified genes might be find a clinical application as markers for the processes occurring through the female reproductive system.

Material and methods

Patient selection and granulosa cell separation

The follicular fluid with GCs were obtained from patients who received *in vitro* fertilization (IVF) therapy at the Department of Infertility and Reproductive Endocrinology, Poznan University of Medical Sciences. The study group consisted of eight women aged 18–40 with diagnosed infertility. The exclusion criteria were established according to Bologna's criteria of poor ovarian responders, which was published by the European Society of Human Reproduction and Embryology (ESHRE) in 2011 [8].

During the treatment all patients exhibiting previously diagnosed infertility were subjected to the procedure of controlled ovarian hyperstimulation performed with human recombinant FSH (Follicle-stimulating hormone; Gonal-F, Merck Serono, Darmstadt, Germany) and highly purified hMG-HP (Highly purified human menopausal gonadotropin; Menopur, Ferring, Saint-Prex, Switzerland). Injections with cetrorelix acetate were used to supres pituitary function (Cetrotide, Merck Serono, Darmstadt, Germany) Induction of an ovulation through the subcutaneous injection of 6500 U of human chorionic gonadotropin (hCG; Ovitrelle, Merck-Serono, Darmstadt, Germany) was an important experimental intervetions. At the time of transvaginal ultrasound-guided oocyte pick-up (OPU), 36 hours after human chorionic gonadotropin administration the follicles containing GCs from each ovary were collected for further analysis. The FF was collected only from ovarian follicles larger than 16 mm. In an attempt to obtain a GC-containing pellet, the fresh follicular fluid was centrifuged for 10 min at 200 × *g.*

This study was performed according to the tenets of the Declaration of Helsinki for research involving human subjects. The Poznan University of Medical Sciences Bioethical Committee gave approval for the study under resolution 558/17. All participants of study met assumed criteria and gave written informed consent for the research.

Primary cell culture

After collection of hGCs derived from patients undergoing IVF, pellet containing hGCs was washed twice in culture medium by centrifugation at 200 × *g* for 10 min at room temperature. The applied medium consisted of Dulbecco's Modified Eagle Medium (DMEM, Sigma; Merck KGaA, Darmstadt, Germany), 10% fetal bovine serum (FBS, Sigma; Merck KGaA, Darmstadt, Germany), 10 mg/mL gentamicin (Invitrogen; Thermo Fisher Scientific, Inc., Waltham, MA, USA), 4 mM L-glutamine (stock 200 mM, Invitrogen; Thermo Fisher Scientific, Inc., Waltham, MA, USA), 10,000 µg/mL streptomycin, and 10,000 U/mL penicillin (Invitrogen; Thermo Fisher Scientific, Inc., Waltham, MA, USA). The maintained conditions for cell culture in incubator were 37 °C and 5% CO_2 (aerobic conditions). Once, adherent cells reached 90% confluency, they were detached from the flasks using 0.05% trypsin- ethylenediaminetetraacetic (trypsine – EDTA Invitrogen; Thermo Fisher Scientific, Inc., Waltham, MA, USA) for 1–2 min and counted and checked for their viability using the ADAM Automatic Cell Counter (NanoEnTek, Waltham, MA, USA).

The cells have been culture 30 days. The cell culture media was changed twice per week. The next step was to isolate the total RNA from culture dishes.

RNA isolation

Total RNA was isolated from the hGCs after 24h hours, 7 days, 15 days and 30 days of culture on the basis of the Chomczyński–Sacchi method [9]. The harvested GCs were suspended in 1 ml of monophase solution of phenol and guanidine thiocyanate (TRI Reagent®, Sigma-Aldrich, St. Luis, MO, USA). In order to obtain three separate phases, chloroform was added and the vial was centrifuged for 10 min at 12,000 × *g at 4* °C. After this step, the RNA was located in the uppermost aqueous phase. Then, the

phase containing RNA was exposed with 2-propanol (Sigma; Merck KGaA St. Luis, MO, USA; catalog number I9516) and washed with 75% ethanol to precipitate and condense the ribonucleic acid. After the process of isolation samples were used for further analysis. To evaluate the total mRNA amount the optical density at 260 nm was determined using spectrophotometry (NanoDrop spectrophotometer, ThermoScientific, Poland). The mRNA purity was estimated using a 260/280 nm absorption ratio. Samples with a 260/280 absorbance ratio greater than 1.8 were used in the study.

Microarray expression and statistical analysis

Double-stranded cDNA was obtained from 100ng of total RNA with the use of Ambion® WT Expression Kit (Ambion, Austin, TX, USA). Using *in vitro* transcription of the double-stranded cDNA template (GeneChipTM 3'IVT PLUS Reagent Kit, Applied BiosystemsTM, Foster City, CA, USA), tagged complementary RNA (cRNA) was created and amplified in the following step. Divalent cations and temperature were used for the fragmentation of the obtained cRNA. Human Genome U219 Array Strip (Applied BiosystemsTM, Foster City, CA, USA) was hybridized with fragmented and tagged cRNA (7.5 g) at 45 °C for 16 hours. Using the Affymetrix GeneAtlas Fluidics Station, the microarrays were then washed and dyed in accordance with the technical protocol. The Imaging Station of the GeneAtlas System was then used to scan the array strips. Affymetrix GeneAtlas™ Operating Software was used to conduct a preliminary examination of the scanned chips. The software's quality control criteria were used to evaluate the gene expression data's quality. The downstream data analysis software was used to import the obtained CEL files. The R programming language (v. 4.0.3) and Bioconductor (v. 3.16) were used to create all of the analyses and graphs that were presented [10,11]. A description file was combined with each CEL file. We applied the Robust Multiarray Averaging (RMA) technique to correct background, standardize, and summarize data.

The empirical Bayes method's moderated t-statistics were used to determine the statistical significance of the genes under study. Using Benjamini and Hochberg's false discovery rate, the obtained p-value was adjusted for multiple comparisons. Adjusted p-values lower than 0.05 and expression fold changes of more than |2| were used to determine which genes' expression had changed significantly. Differentially expressed genes were subjected to the selection of genes involved in activation of hormonal signaling pathways, cholesterol synthesis and lipids metabolism. The DAVID software (Database for Annotation, Visualization, and Integrated Discovery) was used to obtain the GO BP terms: cholesterol biosynthetic process (GO:0006695); regulation of lipid biosynthetic process (GO:0046890); regulation of lipid metabolic process (GO:0019216); response to insulin (GO:0032868); response to lipopolysaccharide (GO:0032496) from the differentially expressed gene list [12]. These gene expression data were submitted to a hierarchical clustering process, and the results were displayed as a heatmap graph. Using the "GOplot" library, detailed analyses of genes associated with particular GO BP keywords were displayed as graphs.

Additionally, the STRING software analysis (Search Tool for Retrieval of Interacting Genes/Proteins; version 11) was applied to differentially expressed genes from the chosen GO BP terms to predict the interactions between their protein products [13].

Results

Microarray analysis

The primary GCs were collected after 7-day (7D), 15-day (15D), and 30-day (30D) of cultivation. The transcriptomic profile of gene expression was compared to the control group (1-day- 24H). The general profile of the transcriptome changes across experimental groups is presented as **table 1**, with their corresponding p-values at 7-day, 15-day and 30-day vs. the 1-day of the experiment. It has been demonstrated that, for all analyzed groups, the highest fold expression change was observed for *CCL20, CXCL5, MSMO1, and AADAC*.

In the following analysis step, the gene expression pattern was compared and overlayed on biological processes (GO processes) across all analyzed groups and presented as a heatmap (**Fig. 1-5**). The first heatmap presents differentially expressed genes related to cholesterol biosynthetic process (**Fig. 1**). It has been revealed that gene expression follows a specific pattern, with almost all gene expressions decreasing with the duration of the experiment. Only two genes, *APOE* and *APOA1* demonstrate no changes in expression profile at 7-day and 15-day of the experiment compared to control, with decreased expression at 30-day. It is worth indicating that the expression of *APOE* and *APOA1* diverges from other genes from the beginning of the experiment.

The gene expression profile revealed maintained upregulation of lipid biosynthesis. Nevertheless, there were several genes, namely *PROX1, DGAT2, SREBF1*, and *XB1,* that showed downregulation compared to control (**Fig. 2**). Similarly to the analysis of genes related to cholesterol biosynthesis, the expression of *APOE*, *APOC1*, *APOA1*, *ATP1A1*, and *ACADVL* were upregulated in 7-, and 15-day compared to control.

Next, the analysis of genes involved in regulation of lipid metabolism processes has been performed (**Fig. 3**). It has been indicated that the expression of *OPA3*, *PPARA*, *PPARG*, *PROX1*, and *SEC14L2* was decreased across all the experimental groups compared to control. Moreover, analysis of genes as-

TABLE 1 The LogFC of expression, adj. P. values, and ENTREZ gene IDs of genes of interest described in this manuscript

GENE		LOG2 FC			ADJ. P. VALUE		
NAME	**ENTREZ ID**	**D7 VS. D1**	**D15 VS. D1**	**D30 VS. D1**	**D7 VS. D1**	**D15 VS. D1**	**D30 VS. D1**
CCL20	6364	7,76	7,70	7,65	$4,07*10^{-4}$	$3,74*10^{-4}$	$3,03*10^{-4}$
CXCL5	6374	6,64	6,72	6,99	$5,13*10^{-4}$	$4,53*10^{-4}$	$3,03*10^{-4}$
MSMO1	6307	5,31	5,47	4,73	$7,67*10^{-3}$	$6,30*10^{-3}$	$8,68*10^{-3}$
AADAC	13	5,17	3,30	5,02	$2,58*10^{-3}$	$8,42*10^{-3}$	$2,14*10^{-3}$
KL	9365	4,69	4,86	4,70	$9,10*10^{-5}$	$6,16*10^{-5}$	$6,50*10^{-5}$
PTGS2	5743	4,50	4,54	4,79	$9,56*10^{-4}$	$8,93*10^{-4}$	$6,17*10^{-4}$
IL24	11009	4,22	4,19	4,32	$3,93*10^{-3}$	$3,72*10^{-3}$	$2,92*10^{-3}$
HMGCS1	3157	3,99	4,53	3,98	$1,16*10^{-2}$	$6,84*10^{-3}$	$9,07*10^{-3}$
PID1	55022	3,72	3,87	3,81	$2,44*10^{-3}$	$2,04*10^{-3}$	$1,68*10^{-3}$
DCN	1634	3,63	3,06	4,00	$3,44*10^{-1}$	$4,07*10^{-1}$	$2,56*10^{-1}$
IRAK3	11213	3,63	3,44	3,65	$3,63*10^{-2}$	$3,81*10^{-2}$	$2,89*10^{-2}$
PPBP	5473	3,16	3,23	3,23	$2,11*10^{-3}$	$1,73*10^{-3}$	$1,38*10^{-3}$
IDI1	3422	3,00	3,49	2,48	$2,26*10^{-2}$	$1,25*10^{-2}$	$3,26*10^{-2}$
NAMPT	10135	2,93	2,40	2,89	$4,52*10^{-3}$	$7,57*10^{-3}$	$3,59*10^{-3}$
PDE4B	5142	2,82	2,81	2,68	$2,85*10^{-4}$	$3,26*10^{-4}$	$2,71*10^{-4}$
CXCL3	2921	2,73	2,90	2,78	$3,08*10^{-3}$	$2,50*10^{-3}$	$2,34*10^{-3}$
LDLR	3949	2,69	3,26	2,57	$1,29*10^{-2}$	$6,33*10^{-3}$	$1,17*10^{-2}$
S100A8	6279	2,62	2,92	2,99	$1,58*10^{-3}$	$1,13*10^{-3}$	$8,16*10^{-4}$
NSDHL	50814	2,61	2,73	2,52	$1,86*10^{-3}$	$1,48*10^{-3}$	$1,46*10^{-3}$
HSD17B7	51478	2,60	2,50	2,33	$4,50*10^{-3}$	$4,62*10^{-3}$	$4,94*10^{-3}$
GCLC	2729	2,53	2,11	3,15	$2,34*10^{-3}$	$3,43*10^{-3}$	$9,32*10^{-4}$
HMGCR	3156	2,40	2,99	2,56	$9,87*10^{-3}$	$4,44*10^{-3}$	$6,21*10^{-3}$
FADS1	3992	2,38	2,46	2,26	$3,59*10^{-3}$	$3,10*10^{-3}$	$3,27*10^{-3}$
SCARB1	949	2,35	2,09	2,50	$2,00*10^{-3}$	$2,50*10^{-3}$	$1,19*10^{-3}$
FDPS	2224	2,31	2,38	2,24	$6,41*10^{-3}$	$5,32*10^{-3}$	$5,48*10^{-3}$
WNT5A	7474	2,29	1,74	2,15	$5,75*10^{-2}$	$1,09*10^{-1}$	$5,64*10^{-2}$
PDE4D	5144	2,19	3,17	3,24	$4,80*10^{-2}$	$1,37*10^{-2}$	$1,16*10^{-2}$
LGALS12	85329	2,11	2,27	2,93	$8,63*10^{-2}$	$6,21*10^{-2}$	$2,69*10^{-2}$
TFPI	7035	2,01	1,27	1,47	$4,33*10^{-3}$	$1,60*10^{-2}$	$9,01*10^{-3}$
SQLE	6713	1,88	1,93	1,81	$3,20*10^{-2}$	$2,67*10^{-2}$	$2,95*10^{-2}$
CXCL1	2919	1,87	1,47	2,27	$2,47*10^{-1}$	$3,43*10^{-1}$	$1,39*10^{-1}$
NFKBIA	4792	1,87	1,72	1,84	$6,04*10^{-2}$	$6,74*10^{-2}$	$5,13*10^{-2}$
PPARG	5468	1,86	2,15	2,87	$1,23*10^{-2}$	$6,84*10^{-3}$	$2,50*10^{-3}$
CITED1	4435	1,85	2,04	2,05	$1,37*10^{-3}$	$9,94*10^{-4}$	$7,76*10^{-4}$
SERPINA3	12	1,80	1,87	1,81	$4,73*10^{-3}$	$3,89*10^{-3}$	$3,54*10^{-3}$
SC5D	6309	1,68	2,06	1,57	$2,02*10^{-2}$	$9,53*10^{-3}$	$2,02*10^{-2}$
EBP	10682	1,67	2,36	2,34	$2,26*10^{-2}$	$6,96*10^{-3}$	$6,26*10^{-3}$
CYP51A1	1595	1,65	1,74	1,50	$6,59*10^{-3}$	$5,13*10^{-3}$	$7,02*10^{-3}$
CD14	929	1,63	1,85	1,49	$1,58*10^{-1}$	$1,04*10^{-1}$	$1,64*10^{-1}$
FDFT1	2222	1,63	1,78	1,53	$2,17*10^{-2}$	$1,46*10^{-2}$	$2,12*10^{-2}$
INSR	3643	1,37	0,31	0,90	$4,90*10^{-2}$	$6,20*10^{-1}$	$1,24*10^{-1}$
CXCL8	3576	1,33	1,12	1,15	$9,90*10^{-2}$	$1,34*10^{-1}$	$1,20*10^{-1}$

GENE		LOG2 FC			ADJ. P. VALUE		
NAME	**ENTREZ ID**	**D7 VS. D1**	**D15 VS. D1**	**D30 VS. D1**	**D7 VS. D1**	**D15 VS. D1**	**D30 VS. D1**
CREBL2	1389	1,31	1,09	1,18	$5,91*10^{-3}$	$9,38*10^{-3}$	$6,50*10^{-3}$
ABHD6	57406	1,25	1,81	2,12	$4,06*10^{-2}$	$1,17*10^{-2}$	$6,27*10^{-3}$
APOC1	341	1,23	2,41	5,01	$3,74*10^{-1}$	$8,45*10^{-2}$	$8,52*10^{-3}$
ADM	133	1,23	0,22	1,36	$3,63*10^{-2}$	$6,80*10^{-1}$	$2,16*10^{-2}$
MVD	4597	1,18	1,46	1,36	$3,94*10^{-2}$	$1,84*10^{-2}$	$2,10*10^{-2}$
HAMP	57817	1,14	1,09	1,23	$5,21*10^{-3}$	$5,53*10^{-3}$	$3,31*10^{-3}$
PTPN2	5771	1,14	0,96	1,26	$1,28*10^{-2}$	$1,95*10^{-2}$	$7,25*10^{-3}$
MEF2C	4208	1,10	1,76	2,78	$1,77*10^{-1}$	$4,66*10^{-2}$	$1,03*10^{-2}$
EGR1	1958	1,07	1,49	1,16	$2,74*10^{-1}$	$1,24*10^{-1}$	$2,05*10^{-1}$
TLR2	7097	1,07	1,09	1,17	$1,17*10^{-2}$	$9,54*10^{-3}$	$6,80*10^{-3}$
CCL3	6348	1,06	1,03	1,26	$1,00*10^{-2}$	$9,49*10^{-3}$	$4,49*10^{-3}$
XBP1	7494	1,05	0,99	0,82	$5,50*10^{-3}$	$6,06*10^{-3}$	$9,48*10^{-3}$
TNFRSF1B	7133	1,05	1,00	1,15	$1,44*10^{-2}$	$1,46*10^{-2}$	$8,51*10^{-3}$
MVK	4598	1,05	0,90	1,02	$5,85*10^{-3}$	$8,32*10^{-3}$	$4,93*10^{-3}$
RIPK2	8767	1,04	1,26	1,25	$2,04*10^{-1}$	$1,17*10^{-1}$	$1,11*10^{-1}$
C5AR1	728	0,98	1,87	1,81	$2,60*10^{-1}$	$4,93*10^{-2}$	$4,94*10^{-2}$
PPP2R5A	5525	0,97	1,01	0,57	$4,21*10^{-2}$	$3,33*10^{-2}$	$1,46*10^{-1}$
PPARA	5465	0,96	0,81	0,86	$1,29*10^{-2}$	$1,95*10^{-2}$	$1,42*10^{-2}$
PPARA	5465	0,96	0,81	0,86	$1,29*10^{-2}$	$1,95*10^{-2}$	$1,42*10^{-2}$
ATP1A1	476	0,94	0,88	1,62	$4,57*10^{-2}$	$4,98*10^{-2}$	$6,75*10^{-3}$
IFNAR1	3454	0,92	0,69	0,96	$1,41*10^{-2}$	$3,07*10^{-2}$	$9,88*10^{-3}$
PROX1	5629	0,89	0,92	0,93	$4,70*10^{-2}$	$3,79*10^{-2}$	$3,29*10^{-2}$
CCKBR	887	0,88	1,08	0,97	$6,04*10^{-2}$	$2,94*10^{-2}$	$3,64*10^{-2}$
ABCA1	19	0,86	0,61	0,75	$2,37*10^{-2}$	$5,88*10^{-2}$	$2,92*10^{-2}$
DGAT2	84649	0,83	1,00	1,19	$4,08*10^{-2}$	$2,09*10^{-2}$	$1,09*10^{-2}$
ACADVL	37	0,80	0,68	1,04	$1,09*10^{-1}$	$1,47*10^{-1}$	$4,40*10^{-2}$
CNBP	7555	0,72	0,62	0,89	$1,46*10^{-2}$	$2,07*10^{-2}$	$5,95*10^{-3}$
DHCR24	1718	0,63	1,18	1,11	$1,79*10^{-1}$	$2,99*10^{-2}$	$3,31*10^{-2}$
PSAP	5660	0,59	0,46	0,50	$1,25*10^{-1}$	$1,92*10^{-1}$	$1,49*10^{-1}$
PRKCA	5578	0,55	0,84	1,19	$2,39*10^{-1}$	$7,89*10^{-2}$	$2,57*10^{-2}$
MTDH	92140	0,53	0,41	0,26	$1,27*10^{-1}$	$2,00*10^{-1}$	$4,10*10^{-1}$
IRS1	3667	0,51	0,39	1,00	$4,31*10^{-1}$	$5,32*10^{-1}$	$1,02*10^{-1}$
TNFAIP8L3	388121	0,46	0,39	0,34	$1,48*10^{-1}$	$1,90*10^{-1}$	$2,33*10^{-1}$
NFKBIB	4793	0,39	0,63	0,67	$1,90*10^{-1}$	$4,96*10^{-2}$	$3,86*10^{-2}$
OPA3	80207	0,29	0,19	0,29	$2,40*10^{-1}$	$4,30*10^{-1}$	$2,17*10^{-1}$
TJP1	7082	0,19	0,31	0,30	$3,46*10^{-1}$	$1,16*10^{-1}$	$1,19*10^{-1}$
CASP9	842	0,19	0,33	0,19	$3,74*10^{-1}$	$1,13*10^{-1}$	$3,13*10^{-1}$
SNCA	6622	0,15	1,11	1,69	$9,03*10^{-1}$	$2,14*10^{-1}$	$7,24*10^{-2}$
APOE	348	0,13	1,28	4,77	$9,66*10^{-1}$	$5,55*10^{-1}$	$4,07*10^{-2}$
EDF1	8721	0,11	0,16	-0,02	$7,07*10^{-1}$	$5,15*10^{-1}$	$9,53*10^{-1}$
LPIN1	23175	0,06	0,11	0,14	$8,80*10^{-1}$	$7,64*10^{-1}$	$6,69*10^{-1}$
MAPK14	1432	-0,10	0,04	-0,01	$5,77*10^{-1}$	$8,32*10^{-1}$	$9,40*10^{-1}$
ABHD5	51099	-0,13	0,67	0,23	$8,40*10^{-1}$	$1,72*10^{-1}$	$6,45*10^{-1}$
APOA1	335	-0,44	2,24	3,94	$7,79*10^{-1}$	$9,40*10^{-2}$	$1,63*10^{-2}$

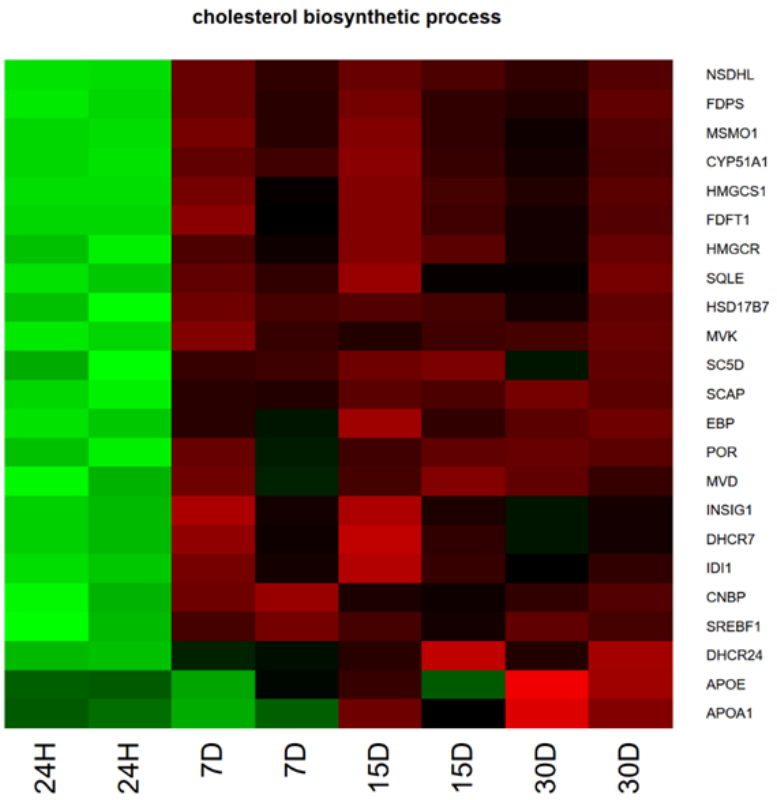

FIGURE 1 Expression heatmap of genes associated to cholesterol biosynthetic process (GO:0006695) in all analyzed groups. Expression values are scaled by rows and presented as colors and range from dark red (downregulation) to dark green (upregulation)

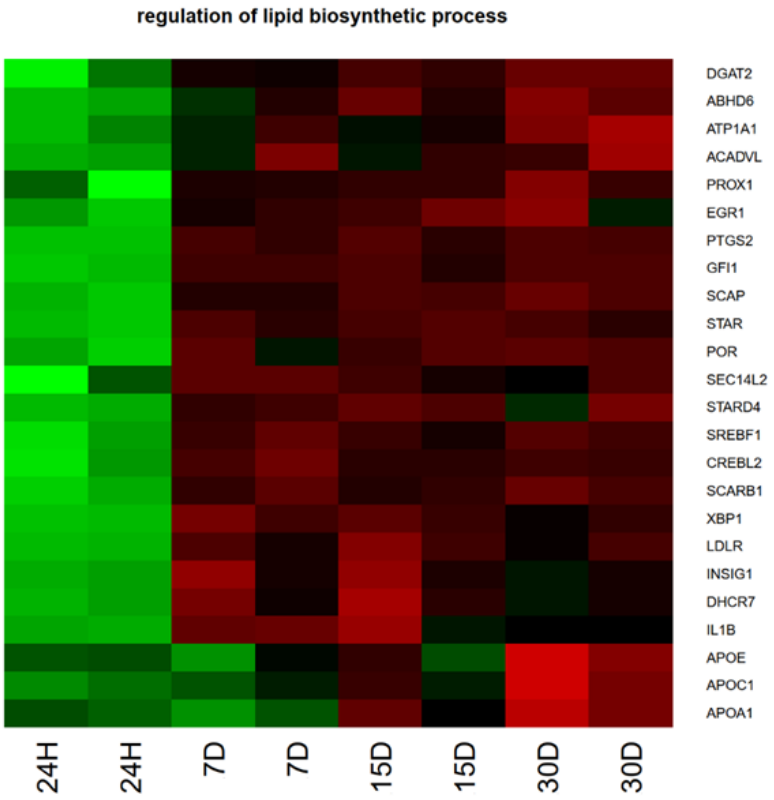

FIGURE 2 Expression heatmap of genes associated to regulation of lipid biosynthetic process (GO:0046890) in all analyzed groups. Expression values are scaled by rows and presented as colors and range from dark red (downregulation) to dark green (upregulation)

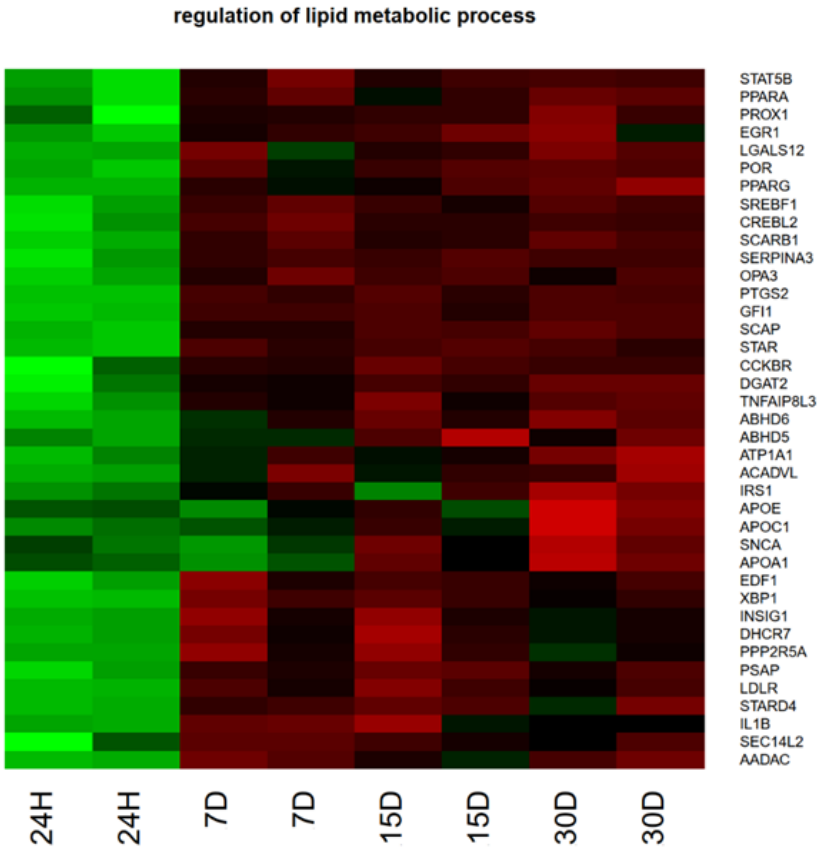

FIGURE 3 Expression heatmap of genes associated to regulation of lipid metabolic process (GO:0019216) in all analyzed groups. Expression values are scaled by rows and presented as colors and range from dark red (downregulation) to dark green (upregulation)

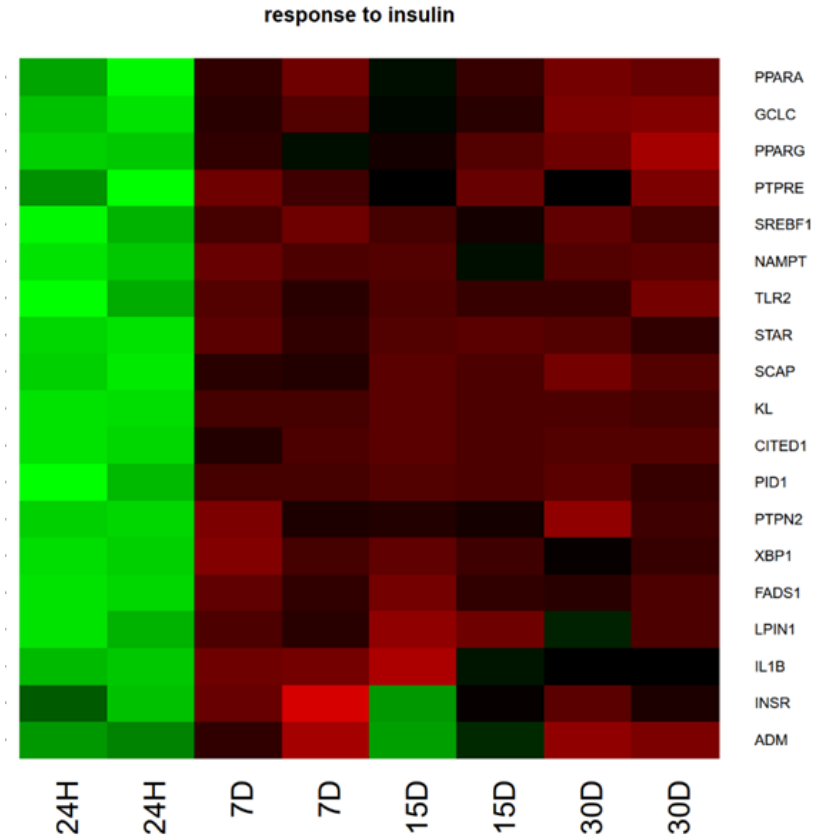

FIGURE 4 Expression heatmap of genes associated to response to insulin biological process (GO:0032868) in all analysed groups. Expression values are scaled by rows and presented as colours and range from dark red (downregulation) to dark green (upregulation)

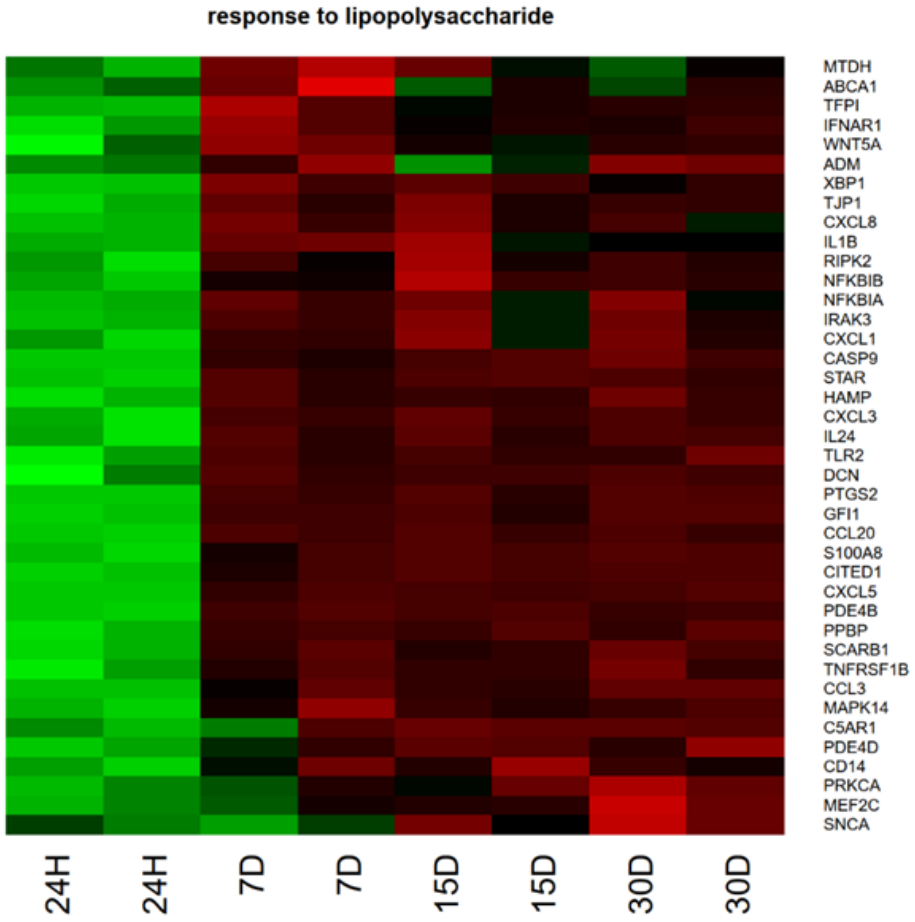

FIGURE 5 Expression heatmap of genes associated to response to lipopolysaccharide biological process (GO:0032496) in all analysed groups. Expression values are scaled by rows and presented as colours and range from dark red (downregulation) to dark green (upregulation)

sociated with response to insulin reveled that the expression of *PPARA*, *SREBF1*, *PTPN2*, and *PTPRE* were decreased in all groups. Only the expression of *INSR* and *ADM* were increased in 15-day compared to the control (**Fig. 4**). Meanwhile, analysis of genes involved in response to lipopolysaccharides revealed that *TFPI*, *CCL3*, *CD14*, and *CXCL5* were downregulated compared to the control (**Fig. 5**). In conclusion, the expression profile follows a specific pattern, showing commonly up and down regulated genes in all analyzed groups.

Next, 29 differentially expressed genes (**Fig. 6**) and their involvement in selected biological processes, such as cholesterol biosynthetic process (GO:0006695); regulation of lipid biosynthetic process (GO:0046890); regulation of lipid metabolic process (GO:0019216); response to insulin (GO:0032868); response to lipopolysaccharide (GO:0032496) were evaluated.

As can be seen, five genes, namely *IL1B, SCAP, SREBF1, STAR, and XBP1,* belonged to four out of five GOs of interest. Furthermore, *APOA1, APOE, DHCR7, GFI1, INSIG, POR,* and *SCARB1* were member of at least three of the analyzed GOs. There were 17 more genes, indicated in **figure 6**, which participated in two GOs of interest, with the rest only being members of one GO.

STRING analysis

Further examination with the Search Tool for the Retrieval of Interacting Genes (STRING) database allowed to identify the direct protein-protein interaction (PPI) network between *SREBF1* and 10 different proteins (**Fig. 7**). *SREBF1* as the center node was associated with: proteins responsible for lipid metabolism PPARA (Peroxisome proliferator-activated receptor alpha), *STAR* (Steroidogenic acute regulatory protein, mitochondrial) and *STARD4* (StAR-related lipid transfer protein 4*),* also for cholesterol biosynthesis process as *IDI1* (Isopentenyl-diphosphate Delta-isomerase 1), *CYP51A1* (Lanosterol 14-alpha demethylase), *SQLE* (Squalene monooxygenase), *HMGCS1* (Hydroxymethylglutaryl-CoA synthase, cytoplasmic) and *FDFT1* (Squalene synthase)*;* next, transport of cholesterol into cells by endocytosis *LDLR* (Low-density lipoprotein receptor); regulation of bile acid biosynthesis STAR, STARD4, and Nuclear receptor that binds peroxisome prolif-

FIGURE 6 A heatmap visualizing enrichment of the analyzed GO categories, as well as the overlap of genes contained within the ontology groups. Enrichment is presented above the table, with a darker color (orange) representing a higher number of genes in the described GO. In turn, the darker the shade of color next to the gene name, the more of the analyzed GOs this gene is the member of. The names of the GOs were presented as abbreviations: CBP - cholesterol biosynthetic process (GO:0006695); RoLBP- regulation of lipid biosynthetic process (GO:0046890); RoLMP - regulation of lipid metabolic process (GO:0019216); RTI - response to insulin (GO:0032868); RTL response to lipopolysaccharide (GO:0032496). The genes participating only in one GO were excluded from the figure

erators such as hypolipidemic drugs and fatty acids PPARG (Peroxisome proliferator-activated receptor gamma). The line thickness in **figure 7** indicates the strength of data support from the sources of text mining and experiments with a cut-off value of highest confidence (0.9).

Discussion

The interactions between oocyte and somatic cells in follicular niche are crucial for formation of high-quality oocytes. Interactions involve endocrine, paracrine and autocrine regulations as well as response to growth and metabolic factors. Further-

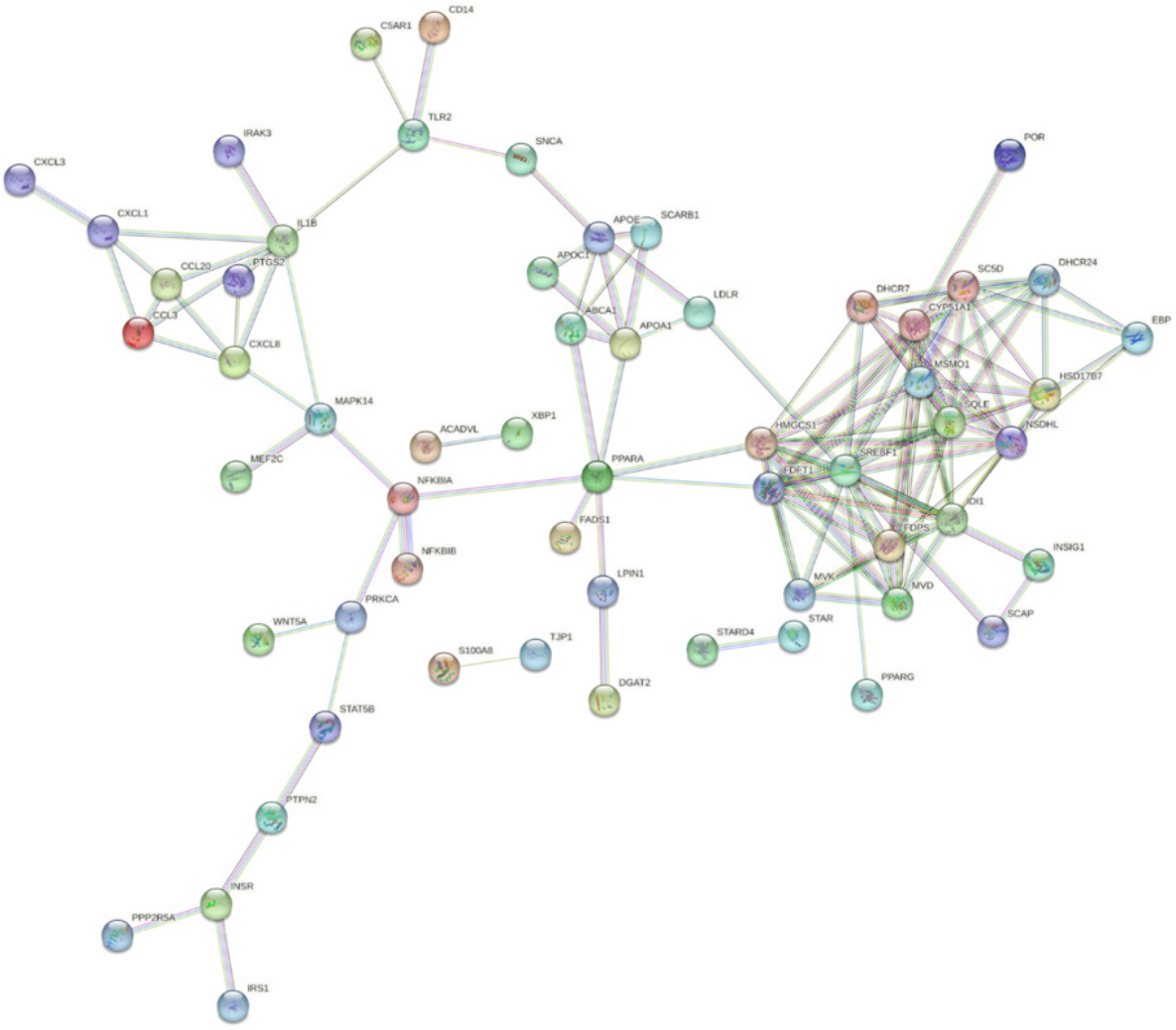

FIGURE 7 The protein-protein interaction showed by Search Tool for the Retrieval of Interacting Genes (STRING) based on analysis of mostly expressed genes. Interacting nodes are displayed in coloured circles. Map key: pink - experimentally determined; blue - from current data bases; dark blue - protein homology; black - co-expression; green – textmining. The analysis was performed using the following settings: Network type: full STRING network; meaning of network edges: evidence; active interaction sources: all; minimum required interaction score: highest confidence (0.900); hide disconnected nodes in the network

more steroid levels in follicular fluid may be useful to predict suitability of an oocyte for IVF [14,15]. GCs fulfil many roles. Their hormonal activity, production of sex hormones such as estradiol during follicular growth, and secretion of progesterone after ovulation is well known and understood [14–18].

The results from microarray analysis shown the changes in expression of genes that are part of five inspected ontological groups:

- cholesterol biosynthetic process (GO:0006695)
- regulation of lipid biosynthetic process (GO:0046890)
- regulation of lipid metabolic process (GO:0019216)
- response to insulin (GO:0032868)
- response to lipopolysaccharide (GO:0032496)

The first 24 hours of GCs *in vitro* primary culture were crucial for further observations. Based on obtained results the pattern of expression can be seen and defined as fairly unified for almost all the genes, with upregulation at day 1 (24 hours) and general downregulation through the other days. Among all genes included in this study some of them stood out during further cultivation.

As mentioned in results section, *APOE* expression pattern diverges from other genes from the beginning of the experiment. *APOE* (apolipoprotein E) is biologically involved in cholesterol, steroid metabolism and lipid transport. It is a major apoprotein of the chylomicron and has an essential role in catabolism of triglyceride-rich lipoprotein constituents. Moreover *APOE* stands out from other lipoproteins because it takes part in lipoproptein-me-

diated distribution of lipids among tissues and has a critical role for maintaining the lipid homeostasis [19,20]. The local production of apoE is commonly associated with steroidogenic tissues, such as ovary [21,22]. It was proven that primary hGCs expressed apoE mRNA among other curcial lipoproteins such as apoB, microsomal triglyceride transfer protein [23]. The significant levels of apoE mRNA were observed in theca cells of ovarian atretic follicles [21]. Thus, apoE inhbits androgen synthesis and is as an important factor involved in regulating steroidogenesis. Additionally *APOA1* is gene encoding apolipoprotein A-I – the major protein component of HDL (high density lipoprotein). Defects in this gene cause diseases associated with HDL deficiencies [24,25].

Another gene, which transcript was upregulated in 7- and 15-day of cultivation is *ACADVL (*also known as *VLCAD)* encoding an enzyme, acyl-coenzyme A dehydrogenase very long chain, involved in fatty acid β-oxidation (FAO) [26]. It was documented that *ACADVL* deficiency reduces myocardial fatty acid beta-oxidation and is associated with cardiomyopathy [27]. Based on a study conducted on human preeclamptic placenta and pregnant mice model, it was suggested that during the hypoxic conditions the expression of FAO-related genes, such as *ACADVL* increased suggesting that expression of FAO-related genes is regulated by hypoxic conditions and directly affects the maternal gluconeogenesis during pregnancy and occurrence of preeclampsia [28]. The upregulation of this gene, is probably related to enhanced activity of metabolic processes during long-term *in vitro* culture.

In the presented study have been shown that the highest fold expression change of *CCL20* and *CXCL5*. *CCL20* gene encodes a protein, which acts as a ligand for C-C chemokine receptor CCR6 [29]. Recently, Duan et al. [30] showed that CCR6-CCL20 axis may represent an important factor in directing sperm-oocyte interaction. They pointed out, that GCs as well as human oocytes represent an abundant source of the CCR6-specific ligand CCL20 and CCL20 protein induces chemotactic responses of human sperm. *CCL20* is also associated with events occurring after ovulation in human follicle. The changes in the ovulated follicle include among others increased action of immune cells and increased expression of granulosa cells' cytokines – IL-6, CCL20, CXCR4 [31]. In reproduction studies area, CXCL5 was investigated as senescence-associated secretory phenotype (SASP) factor partially responsible for embryo implantation failure in human and mouse models. Kawagoe et al. suggested that CXCL5-CXCR2 signalling suppression in blastocyst could be the basis to improve embryo development and pregnancy outcome in middle-aged infertile patients [32].

Among genes associated with pathways of cholesterol biosynthesis and metabolism *MSMO1* and *AADAC* stood out. *MSMO1* (methylsterol monooxygenase 1) encodes a sterol-C4-mehtyl oxidase-like protein, which isolated based on its similarity to the yeast ERG25 protein. MSMO1 protein is localized in ER membrane and plays role in process of cholesterol biosynthesis. Its expression was also proven recently in research on novel regulatory factors in the hypothalamic-pituitary-ovarian axis (HPO) of hens [33]. Arylacetamide deacetylase (gene *AADAC)* is showed an activity of cellular triglyceride lipase and increases the level of intracellular fatty acids from the hydrolysis of newly formed triglyceride reserves, and also participates in the formation of very low-density lipoproteins [34]. *AADAC* annotations in GO include *"*hydrolase activity" and *"*triglyceride lipase activity*"* which are directly related with GO groups.

Cholesterol is transported form the outer mitochondrial membrane to the inner one. This process takes part in mitochondria due to the function of cytochrome P450scc, encoded by *CYP11A1*, gene expressed in steroidogenic tissues such as adrenal cortex, ovarian granulosa cells, testicular Leydig cells, and placenta and other skin, heart, and brain [35]. The enriched tissue expression cluster for STAR gene are also endocrine tissues, which is mainly adrenal gland but also female ovary and testis in male [36,37]. A recent study suggests that downregulation of *STAR and STARD4,* genes associated with regulation of lipid biosynthetic metabolic processes [38]. Downregulation of these genes it might be connected to the fact that *in vitro* culture conditions do not fully reflect the physiological ovarian follicle environment.

Additionally, *PPARG* (encoding peroxisome proliferator-activated receptor gamma) was one of the genes with decreased expression across all experimental groups compared to control. PPAR-gamma is known as regulator of cellular lipid metabolism and adipocyte differentiation [39]. Studies in miceshowed that decreased *PPARG* expression is related to perigonadal-specific fat deposition and insulin sensitivity [40]. PPAR-gamma also plays a key role in regulation of energy balance, lipoprotein metabolism, oxidative stress, and inflammatory signalling [41]. In contrast, PPAR-gamma protein expression level in GCs was determined as factor not directly correlated to the success pregnancy [42].

The description above appeal mainly to the ontological groups associated with lipid and steroid metabolism and biosynthesis. Nevertheless, there are also other areas to pay attention on, such as "response to insulin" and "response to lipopolysaccharides". *ADM* (encodes a hormone - adrenomedullin) with *INSR* (insulin receptor) exhibit increased expression in 15-day compared to the control group during cell culture. *ADM* expression is present in adipose tissue and has an important role in vasodilation, regulation of hormone secretion, promotion of angiogenesis [43]. Considering the recent results [44]

ADM may be applied in future as a pathophysiologic substance in pregnancy-induced hypertension (PIH).

Moreover previous studies have reported that insulin signaling, which includes *INSR* gene is essential for folliculogenesis, granulosa cell differentiation and ovulation and insulin resistance is one of the significant aberrations in polycystic ovarian syndrome (PCOS) [45–47].

Conclusions

To conclude, this microarray analysis suggests that GCs in primary *in vitro* cell culture conditions express steroidogenic markers. The analysis of molecular pathways and its associations in lipid synthesis and metabolism, response to lipoproteins and insulin might outline their significance. Make it possible to connect significant aberrations in certain genes to their roles on cellular level and translate it to clinical observations. Considering the worldwide problems with female fertility and the appearance of new occupational origins of diseases associated with reproductive systems, it is valid to develop new strategies enhancing assisted reproductive techniques in future medicine.

Ethical approval

The study was conducted in accordance with the Declaration of Helsinki, and approved by the Bioethics Committee of Poznan University of Medical Sciences number 558/17.

Acknowledgments

None.

Corresponding author

Wiesława Kranc, Department of Anatomy, Poznan University of Medical Sciences, Poznań, Poland, e-mail: wkranc@ump.edu.pl.

Conflicts of interest

The authors declare they have no conflict of interest.

References

1. West ER, Shea LD, Woodruff TK. Engineering the follicle microenvironment. Semin Reprod Med. 2007;25(4):287–99; DOI:10.1055/S-2007-980222.
2. Dumesic DA, Meldrum DR, Katz-Jaffe MG, Krisher RL, Schoolcraft WB. Oocyte environment: follicular fluid and cumulus cells are critical for oocyte health. Fertil Steril. 2015;103(2):303–16; DOI:10.1016/j.fertnstert.2014.11.015.
3. Richards JAS. Theca cells. Encycl Reprod. 2018;14–20; DOI:10.1016/B978-0-12-801238-3.64624-X.
4. De Matos DG, Miller K, Scott R, Tran CA, Kagan D, Nataraja SG, Clark A, Palmer S. Leukemia inhibitory factor induces cumulus expansion in immature human and mouse oocytes and improves mouse two--cell rate and delivery rates when it is present during mouse in vitro oocyte maturation. Fertil Steril. 2008;90(6):2367–75; DOI:10.1016/J.FERTNSTERT.2007.10.061.
5. Urs DBS, Wu WH, Komrskova K, Postlerova P, Lin YF, Tzeng CR, Kao SH. Mitochondrial function in modulating human granulosa cell steroidogenesis and female fertility. Int J Mol Sci. 2020;21(10); DOI:10.3390/IJMS21103592.
6. Cole TJ, Short KL, Hooper SB. The science of steroids. Semin Fetal Neonatal Med. 2019;24(3):170–5; DOI:10.1016/J.SINY.2019.05.005.
7. Liu T, Qu J, Tian M, Yang R, Song X, Li R, Yan J, Qiao J. Lipid metabolic process involved in oocyte maturation during folliculogenesis. Front Cell Dev Biol. 2022;10; DOI:10.3389/FCELL.2022.806890.
8. Ferraretti AP, La Marca A, Fauser BCJM, Tarlatzis B, Nargund G, Gianaroli L. ESHRE consensus on the definition of "poor response" to ovarian stimulation for in vitro fertilization: the Bologna criteria. Hum Reprod. 2011;26(7):1616–24; DOI:10.1093/humrep/der092.
9. Chomczynski P, Sacchi N. Single-step method of RNA isolation by acid guanidinium thiocyanate-phenol-chloroform extraction. Anal Biochem. 1987;162(1):156–9; DOI:10.1016/0003-2697(87)90021-2.
10. Zhang Y, Szustakowski J, Schinke M. Bioinformatics analysis of microarray data. Methods Mol Biol. 2009;573:259–84; DOI:10.1007/978-1-60761-247-6_15/COVER.
11. Gentleman RC, Carey VJ, Bates DM, Bolstad B, Dettling M, Dudoit S, Ellis B, Gautier L, Ge Y, Gentry J, Hornik K, Hothorn T, Huber W, Iacus S, Irizarry R, Leisch F, Li C, Maechler M, Rossini AJ, Sawitzki G, Smith C, Smyth G, Tierney L, Yang JY, Zhang J. Bioconductor: open software development for computational biology and bioinformatics. Genome Biol 2004 510. 2004;5(10):1–16; DOI:10.1186/GB-2004-5-10-R80.
12. Dennis G, Sherman BT, Hosack DA, Yang J, Gao W, Lane HC, Lempicki RA. DAVID: database for annotation, visualization, and integrated discovery. Genome Biol. 2003;4(5):1–11; DOI:10.1186/GB-2003-4-9-R60/TABLES/3.
13. Szklarczyk D, Gable AL, Lyon D, Junge A, Wyder S, Huerta-Cepas J, Simonovic M, Doncheva NT, Morris JH, Bork P, Jensen LJ, Von Mering C. STRING v11: protein–protein association networks with increased coverage, supporting functional discovery in genome-wide experimental datasets. Nucleic Acids Res. 2019;47(D1):D607–13; DOI:10.1093/NAR/GKY1131.
14. Wen X, Li D, Tozer AJ, Docherty SM, Iles RK. Estradiol, progesterone, testosterone profiles in human follicular fluid and cultured granulosa cells from luteinized pre-ovulatory follicles. Reprod Biol Endocrinol. 2010;8(1):117; DOI:10.1186/1477-7827-8-117.
15. Heiligentag M, Eichenlaub-Ritter U. Preantral follicle culture and oocyte quality. Reprod Fertil Dev. 2017;30(1):18–43; DOI:10.1071/RD17411.
16. Fortune JE. Ovarian production of estradiol: the two-cell, two-gonadotropin model. Encycl Reprod. 2018;165–71; DOI:10.1016/B978-0-12-801238-3.64637-8.
17. Turathum B, Gao EM, Chian RC. The function of cumulus cells in oocyte growth and maturation and in subsequent ovulation and fertilization. Cells. 2021;10(9); DOI:10.3390/CELLS10092292.
18. Kranc W, Budna J, Kahan R, Chachuła A, Bryja A, Ciesiółka S, Borys S, Antosik MP, Bukowska D, Brussow KP, Bruska M, Nowicki M, Zabel M, Kempisty B. Molecular basis of growth, proliferation, and differentiation of mammalian follicular granulosa cells. J Biol Regul Homeost Agents. n.d.;31(1):1–8.
19. Fazio S, Linton MF, Swift LL. The cell biology and physiologic relevance of ApoE recycling. Trends Cardiovasc Med. 2000;10(1):23–30; DOI:10.1016/S1050-1738(00)00033-5.
20. Kockx M, Traini M, Kritharides L. Cell-specific production, secretion, and function of apolipoprotein E. J Mol Med (Berl). 2018;96(5):361–71; DOI:10.1007/S00109-018-1632-Y.
21. Nicosia M, Moger WH, Dyer CA, Prack MM, Williams DL. Apolipoprotein-E messenger RNA in rat ovary is expressed in theca and interstitial cells and presumptive macrophage, but not in granulosa cells. Mol Endocrinol. 1992;6(6):978–88; DOI:10.1210/MEND.6.6.1495495.
22. Polacek D, Beckmann MW, Schreiber JR. Rat ovarian apolipoprotein E: localization and gonadotropic control of messenger RNA. Biol Reprod. 1992;46(1):65–72; DOI:10.1095/BIOLREPROD46.1.65.
23. Gautier T, Becker S, Drouineaud V, Ménétrier F, Sagot P, Nofer JR, Von Otte S, Lagrost L, Masson D, Tietge UJF. Human luteinized granulosa cells secrete apoB100-containing lipoproteins. J Lipid Res. 2010;51(8):2245–52; DOI:10.1194/JLR.M005181.
24. Schaefer EJ, Geller AS, Endress G. The biochemical and genetic diagnosis of lipid disorders. Curr Opin Lipidol. 2019;30(2):56–62; DOI:10.1097/MOL.0000000000000590.
25. Bahrami A, Barreto GE, Lombardi G, Pirro M, Sahebkar A. Emerging roles for high-density lipoproteins in neurodegenerative disorders. Biofactors. 2019;45(5):725–39; DOI:10.1002/BIOF.1541.
26. Souri M, Aoyama T, Yamaguchi S, Hashimoto T. Relationship between structure and substrate-chain-length specificity of mitochondrial very-long-chain acyl-coenzyme A dehydrogenase. Eur J Biochem. 1998;257(3):592–8; DOI:10.1046/J.1432-1327.1998.2570592.X.
27. Xiong D, He H, James J, Tokunaga C, Powers C, Huang Y, Osinska H, Towbin JA, Purevjav E, Balschi JA, Javadov S, McGowan FX, Strauss AW, Khuchua Z. Cardiac-specific VLCAD deficiency induces dilated cardiomyopathy and cold intolerance. Am J Physiol Heart Circ Physiol. 2014;306(3); DOI:10.1152/AJPHEART.00931.2012.
28. Shin E-K, Kang HY, Yang H, Jung E-M, Jeung E-B. The regulation of fatty acid oxidation in human preeclampsia. Reprod Sci. 2016;23(10):1422-33; DOI:10.1177/1933719116641759.
29. Kwantwi LB, Wang S, Sheng Y, Wu Q. Multifaceted roles of CCL20 (C-C motif chemokine ligand 20): mechanisms and communication networks in breast cancer progression. Bioengineered. 2021;12(1):6923; DOI:10.1080/21655979.2021.1974765.

30. Duan YG, Wehry UP, Buhren BA, Schrumpf H, Oláh P, Bünemann E, Yu CF, Chen SJ, Müller A, Hirchenhain J, Van Lierop A, Novak N, Cai ZM, Krüssel JS, Schuppe HC, Haidl G, Gerber PA, Allam JP, Homey B. CCL20-CCR6 axis directs sperm-oocyte interaction and its dysregulation correlates/associates with male infertility‡. Biol Reprod. 2020;103(3):630–42; DOI:10.1093/BIOLRE/IOAA072.
31. Sepuru KM, Poluri KM, Rajarathnam K. Solution structure of CXCL5 - a novel chemokine and adipokine implicated in inflammation and obesity. PLoS One. 2014;9(4); DOI:10.1371/JOURNAL.PONE.0093228.
32. Kawagoe Y, Kawashima I, Sato Y, Okamoto N, Matsubara K, Kawamura K. CXCL5-CXCR2 signaling is a senescence-associated secretory phenotype in preimplantation embryos. Aging Cell. 2020;19(10); DOI:10.1111/ACEL.13240.
33. Li J, Li C, Li Q, Li G, Li W, Li H, Kang X, Tian Y. Novel regulatory factors in the hypothalamic-pituitary-ovarian axis of hens at four developmental stages. Front Genet. 2020;11:1367; DOI:10.3389/FGENE.2020.591672.
34. Nourbakhsh M, Douglas DN, Pu CH, Lewis JT, Kawahara T, Lisboa LF, Wei E, Asthana S, Quiroga AD, Law LMJ, Chen C, Addison WR, Nelson R, Houghton M, Lehner R, Kneteman NM. Arylacetamide deacetylase: a novel host factor with important roles in the lipolysis of cellular triacylglycerol stores, VLDL assembly and HCV production. J Hepatol. 2013;59(2):336–43; DOI:10.1016/J.JHEP.2013.03.022.
35. Arboleda VA, Quigley CA, Vilain E. Genetic basis of gonadal and genital development. Endocrinol Adult Pediatr. 2016;2–2:2051-2085.e7; DOI:10.1016/B978-0-323-18907-1.00118-9.
36. Stocco DM. StAR protein and the regulation of steroid hormone biosynthesis. Annu Rev Physiol. 2001;63:193–213; DOI:10.1146/ANNUREV.PHYSIOL.63.1.193.
37. Sugawara T, Holt JA, Driscoll D, Strauss JF, Lin D, Miller WL, Patterson D, Clancy KP, Hart IM, Clark BJ, Stocco DM. Human steroidogenic acute regulatory protein: functional activity in COS-1 cells, tissue-specific expression, and mapping of the structural gene to 8p11.2 and a pseudogene to chromosome 13. Proc Natl Acad Sci USA. 1995;92(11):4778–82; DOI:10.1073/PNAS.92.11.4778.
38. Kranc W, Brązert M, Ożegowska K, Nawrocki M, Budna J, Celichowski P, Dyszkiewicz-Konwińska M, Jankowski M, Jeseta M, Pawelczyk L, Bruska M, Nowicki M, Zabel M, Kempisty B. Expression profile of genes regulating steroid biosynthesis and metabolism in human ovarian granulosa cells - a primary culture approach. Int J Mol Sci. 2017;18(12):2673; DOI:10.3390/ijms18122673.
39. Hallenborg P, Jørgensen C, Petersen RK, Feddersen S, Araujo P, Markt P, Langer T, Furstenberger G, Krieg P, Koppen A, Kalkhoven E, Madsen L, Kristiansen K. Epidermis-type lipoxygenase 3 regulates adipocyte differentiation and peroxisome proliferator-activated receptor gamma activity. Mol Cell Biol. 2010;30(16):4077–91; DOI:10.1128/MCB.01806-08.
40. Tsai YS, Tsai PJ, Jiang MJ, Chou TY, Pendse A, Kim HS, Maeda N. Decreased PPAR gamma expression compromises perigonadal-specific fat deposition and insulin sensitivity. Mol Endocrinol. 2009;23(11):1787–98; DOI:10.1210/ME.2009-0073.
41. Seiri P, Abi A, Soukhtanloo M. PPAR-γ: Its ligand and its regulation by microRNAs. J Cell Biochem. 2019;120(7):10893–908; DOI:10.1002/JCB.28419.
42. Sahmani M, Najafipour R, Farzadi L, Sakhinia E, Darabi M, Shahnazi V, Mehdizadeh A, Shaaker M, Noori M. Correlation between PPARγ protein expression level in granulosa cells and pregnancy rate in IVF program. Iran J Reprod Med. 2012;10(2):149.
43. Kitamura K, Sakata J, Kangawa K, Kojima M, Matsuo H, Eto T. Cloning and characterization of cDNA encoding a precursor for human adrenomedullin. Biochem Biophys Res Commun. 1993;194(2):720–5; DOI:10.1006/BBRC.1993.1881.
44. Makino Y, Shibata K, Makino I, Kangawa K, Kawarabayashi T. Alteration of the adrenomedullin receptor components gene expression associated with the blood pressure in pregnancy-induced hypertension. J Clin Endocrinol Metab. 2001;86(10):5079–5079; DOI:10.1210/JCEM.86.10.8099.
45. Belani M, Deo A, Shah P, Banker M, Singal P, Gupta S. Differential insulin and steroidogenic signaling in insulin resistant and non-insulin resistant human luteinized granulosa cells-A study in PCOS patients. J Steroid Biochem Mol Biol. 2018;178:283–92; DOI:10.1016/J.JSBMB.2018.01.008.
46. Sekulovski N, Whorton AE, Shi M, Hayashi K, MacLean JA. Insulin signaling is an essential regulator of endometrial proliferation and implantation in mice. FASEB J. 2021;35(4); DOI:10.1096/FJ.202002448R.
47. Daghestani MH, Alqahtani HA, AlBakheet AB, Al Deery M, Awartani KA, Daghestani MH, Kaya N, Warsy A, Coskun S, Colak D. Global transcriptional profiling of granulosa cells from polycystic ovary syndrome patients: comparative analyses of patients with or without history of ovarian hyperstimulation syndrome reveals distinct biomarkers and pathways. J Clin Med. 2022;11(23); DOI:10.3390/JCM11236941.